

# Ferroelectric and relaxor properties of $\text{Pb}(\text{Sc}_{0.5}\text{Nb}_{0.5})\text{O}_3$ : Influence of pressure and biasing electric field

E. L. Venturini, R. K. Grubbs, and G. A. Samara

*Sandia National Laboratories, Albuquerque, New Mexico 87175, USA*

Y. Bing and Z.-G. Ye

*Department of Chemistry, Simon Fraser University, Burnaby, British Columbia, Canada V5A 1S6*

(Received 18 August 2005; revised manuscript received 4 July 2006; published 11 August 2006)

The influences of hydrostatic pressure and biasing electric field on the dielectric properties and phase behavior of a single crystal of the perovskite compound  $\text{Pb}(\text{Sc}_{0.5}\text{Nb}_{0.5})\text{O}_3$  (PSN) have been investigated. On cooling from high temperatures, the crystal first enters a relaxor ( $R$ ) state and then spontaneously transforms to a ferroelectric (FE) phase at a temperature,  $T_c$ , substantially below the peak temperature,  $T_m$ , in the dielectric susceptibility. Based on earlier work on ceramic samples, this behavior suggests substantial chemical (Sc and Nb) disorder at the  $B$  sites. Pressure enhances the  $R$  state with strong indications that the FE phase should vanish at a pressure somewhat higher than the highest pressure reached in the experiments, making the  $R$  state the ground state of the crystal at reduced volume. A significant feature of the temperature ( $T$ )-pressure ( $P$ ) phase diagram is the finding that the  $T_c(P)$  phase line should terminate at a pressure between 10 and 15 kbar in a manner akin to a critical point; however, in the case of PSN this feature represents a FE-to- $R$  crossover. Such behavior suggests that a path can be defined that takes the crystal from the FE phase to the  $R$  state without crossing a phase boundary. A biasing electric field favors the FE phase over the  $R$  state, and the results indicate that the  $R$  state vanishes at  $\geq 5$  kV/cm. The magnitudes of both the high  $T$  Curie-Weiss constant,  $C$ , and the change in entropy (or latent heat) at  $T_c$  are found to be comparable to those of simple displacive perovskite oxides such as  $\text{BaTiO}_3$  and  $\text{PbTiO}_3$ .

DOI: [10.1103/PhysRevB.74.064108](https://doi.org/10.1103/PhysRevB.74.064108)

PACS number(s): 77.80.-e, 77.90.+k, 77.22.-d, 77.84.Dy

## I. INTRODUCTION

Many compositionally disordered  $\text{ABO}_3$  perovskite oxides (where  $A$  and  $B$  denote the  $A$ - and  $B$ -site cations, respectively) exhibit relaxor ferroelectric responses generally characterized by a broad, frequency-dependent peak in the dielectric susceptibility (or dielectric constant,  $\epsilon'$ ), no thermal hysteresis, no, or vanishingly small, remanent polarization, and the absence of a macroscopic-phase (symmetry) change below the peak temperature,  $T_m$ , in  $\epsilon'(T)$ . However, there is symmetry breaking on the nanometer scale leading to the formation of polar nanodomains that exist well above  $T_m$  and that strongly affect the properties.<sup>1,2</sup> Additionally, relaxors possess large  $\epsilon'$ 's, exceptionally large electrostrictive coefficients and large electro-optical constants, properties that are technologically important. Understanding these properties has been a challenging task.

Relaxor behavior is observed in both mixed  $\text{ABO}_3$  oxides such as La- and Ba-substituted PZTs ( $\text{PbZr}_{1-x}\text{Ti}_x\text{O}_3$ ) and  $\text{KTa}_{1-x}\text{Nb}_x\text{O}_3$  with  $x \leq 0.02$ , where the substituents are randomly distributed on the  $A$  or  $B$  sites, and in compounds of the form  $\text{ABB}'\text{O}_3$  (where  $B$  and  $B'$  refer to  $B$ -site cations with different valence).<sup>1,2</sup> Examples of the latter include  $\text{PbMg}_{1/3}\text{Nb}_{2/3}\text{O}_3$  (or PMN) and  $\text{PbSc}_{1/2}\text{Nb}_{1/2}\text{O}_3$  (or PSN). In these crystals the disorder results from having mixed valence ions on the  $B$  site, and there is also an off-center displacement of the  $\text{Pb}^{+2}$  ions.<sup>3-7</sup> PMN is the prototypical classic relaxor that retains its high- $T$  cubic phase down to the lowest temperatures.

PSN and the isomorphic compound  $\text{PbSc}_{1/2}\text{Ta}_{1/2}\text{O}_3$  (or PST), on the other hand, exhibit more complex behavior that

derives from the ability to control the degree of  $B$ -site chemical order. Stenger and Burggraaf determined the kinetics of this ordering<sup>3</sup> and the effects of ordering on the physical properties<sup>8</sup> of PSN and PST ceramic samples. Chu *et al.*<sup>9</sup> prepared and studied two types of high-quality ceramic PSN samples where the degree of order was controlled by proper high-temperature annealing and/or quenching in different atmospheres. It was found that disordered samples (PSN- $D$ ) first enter a relaxor state on cooling followed by a spontaneous (i.e., in the absence of electrical bias) cubic relaxor ( $R$ )-to-rhombohedral ferroelectric (FE) transition. The  $R$ -FE transition at a temperature  $T_c$  is first order, accompanied by discontinuous changes in lattice parameters and thermal hysteresis. The second type of sample was an as-sintered disordered material with Pb vacancies (PSN- $DV$ ) containing  $\sim 5\%$  weight loss due to the loss of volatile Pb during high-temperature processing and exhibited full relaxor character.

Malibert *et al.*<sup>5</sup> investigated PSN- $D$  and PSN- $DV$  single crystals with similar results, and they also studied a highly ordered crystal (PSN- $O$ ) that they anticipated would exhibit "classic ferroelectric" behavior, but found that it still had some relaxorlike character. Synchrotron radiation and neutron-diffraction studies<sup>5,6</sup> have shown that all three types of PSN samples have essentially the same low-temperature crystal structure: rhombohedral space group  $R3m$ . This structure for the FE phase derives from the cubic phase by counter rotations of adjacent oxygen octahedra, as well as cooperative displacements of the Pb and Sc and Nb ions in the same direction along the threefold  $[111]$  axis of the cubic phase. This then becomes the polar axis of the rhombohedral phase.

Yasuda and Fujita<sup>10</sup> studied the effects of pressure and the electric bias field on the dielectric properties and spontaneous polarization of ordered and disordered PSN ceramics.  $\epsilon'(T)$  for both ceramics showed a single maximum at a temperature  $T_m$  that decreased linearly with increasing pressure. In disordered PSN an electric bias field near 5 kV/cm increased  $T_m$  and decreased  $\epsilon'$  at  $T_m$ ; in contrast,  $T_m$  showed a slight decrease and  $\epsilon'$  at  $T_m$  a slight increase in ordered PSN.<sup>10</sup> In a recent paper Szafranski *et al.*<sup>11</sup> reported the changes with pressure in the dielectric properties of a “highly ordered” PSN ceramic. They identify two anomalies in  $\epsilon'(T)$  associated with the relaxor state and the spontaneous  $R$ -FE transition, respectively;  $T_m$ ,  $\epsilon'$  at  $T_m$ , and  $T_c$  decrease linearly with increasing pressure.

In earlier work we have shown that hydrostatic pressure can provide new insights into the phase behavior and ferroelectric-relaxor crossover, in the  $ABO_3$  perovskites. In particular, it was shown that pressure induces a FE-to- $R$  crossover making the relaxor state the ground state of mixed, compositionally disordered perovskites at high pressure (or reduced volume).<sup>2,12</sup> This background and the availability of a single crystal of disordered PSN of suitable dimensions suggested that a high-pressure study of this material could be fruitful. Indeed this has turned out to be the case. We have also investigated the influence of a biasing dc field on these properties. The results, which have provided a detailed view of the dielectric properties and unusual phase behavior of this interesting crystal, are presented and discussed below.

Some key aspects of the present work have been described briefly elsewhere.<sup>13</sup> We shall refer to the contents of Ref. 13 below.

## II. EXPERIMENTAL DETAILS

### A. Sample preparation

Single crystals of  $Pb(Sc_{1/2}Nb_{1/2})O_3$  were grown by a high-temperature solution method using the mixture of  $PbO$  (80 mol %) and  $B_2O_3$  (20 mol %) as the solvent together with the appropriate amounts of  $Sc_2O_3$  and  $Nb_2O_3$ . The crystals were formed upon slow cooling from 1180 °C to 1100 °C. The as-grown crystals exhibited cubic morphology. X-ray powder diffraction patterns of crushed crystals showed no superlattice peaks, indicating a disordered rhombohedral structure (PSN- $D$ ). The sample used in this study was a pseudocubic (001)-oriented platelet (with a thickness of 0.025 cm and an area of 0.034 cm<sup>2</sup>) which was mirror polished with diamond pastes down to 3  $\mu$ m. The (001) faces were vapor deposited with Cr followed by Au thin films for electrical contacts.

### B. Measurements

The crystal was studied by dielectric spectroscopy (ac field strength  $\leq 10$  V/cm) as a function of temperature (300–600 K), frequency ( $10^2$ – $10^6$  Hz), pressure (0–15 kbar), and electric field (0–5 kV/cm). Two pressure apparatuses were used. One is capable of pressure of up to  $\sim 10$  kbar and temperature up to 450 K, using He as the pressure-transmitting medium. The other is capable of pres-

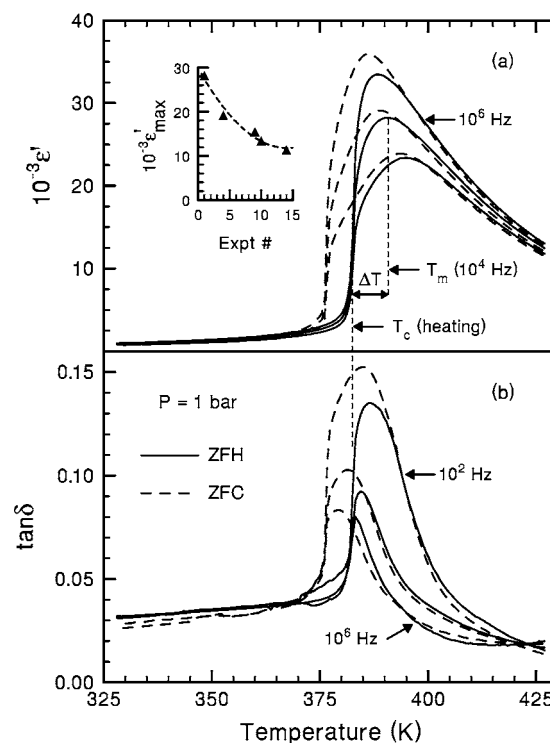


FIG. 1. Thermal hysteresis in  $\epsilon'$  and  $\tan \delta$  (zero-field heating and cooling) for the virgin PSN- $D$  crystal at 1 bar and  $10^2$ ,  $10^4$ , and  $10^6$  Hz.  $T_c$ ,  $T_m$ , and  $\Delta T$  are discussed in the text. The inset shows the degradation of  $\epsilon'_{max}$  with repeated cycling through the ferroelectric transition at  $T_c$ .

ures  $>20$  kbar and temperature from 300–700 K, using a mixture of normal- and iso-pentanes as the pressure-transmitting medium. The temperature was measured with an estimated accuracy of  $\pm 1$  K using chromel and/or alumel thermocouples adjacent to the crystal within the respective pressure cells. The pressure was measured with calibrated-manganin gauges and is estimated to be accurate to  $\pm 4\%$ .

## III. RESULTS AND DISCUSSION

### A. Dielectric properties at 1 bar

The dielectric response of our virgin PSN- $D$  crystal at 1 bar was discussed in Ref. 13, and some key features are shown in Fig. 1. The behavior is very similar to earlier results.<sup>5,9</sup> Briefly, on cooling, the cubic sample first enters the  $R$  state with a peak in the dielectric response at a frequency-dependent  $T_m$ . Upon further cooling, it transforms spontaneously (i.e., without a biasing electric field) into the nondispersive rhombohedral FE phase at  $T_c$ . The FE transition is thermodynamically first order with a 6 K thermal hysteresis. In Fig. 1 the heating data are used to define  $\Delta T = T_m$  (at  $10^4$  Hz)  $- T_c$  which provides a measure of the width of the  $R$  state. The data in Fig. 1 indicate that  $\Delta T$  is larger on cooling than on heating.

Throughout this study, the PSN- $D$  crystal was cycled through the  $R$ -FE phase transition numerous times at 1 bar, at high pressure and at biasing fields. A monotonic decrease in the magnitude of  $\epsilon'$  at  $T_m$  due to cycling was observed,

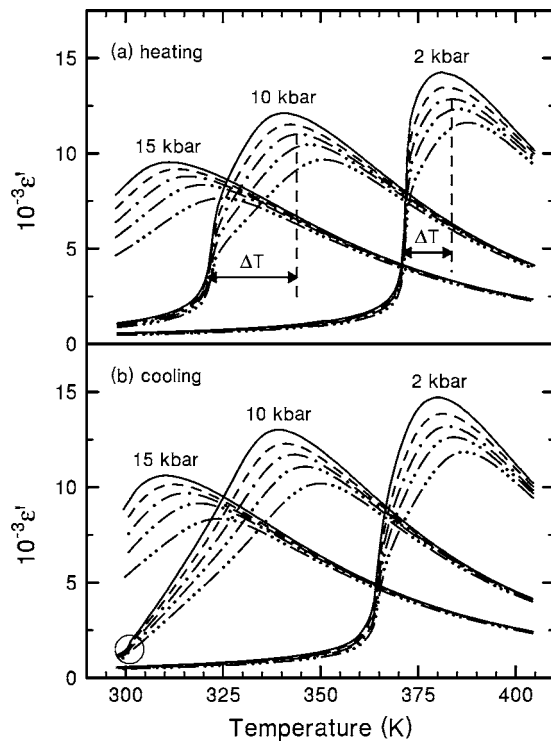


FIG. 2. Heating (a) and cooling (b) isobars of  $\epsilon'(T)$  revealing the influence of hydrostatic pressure on the dielectric response and phase behavior of PSN-*D* (frequencies as shown in Fig. 1). (After Samara and Venturini, Ref. 13, with permission of Phase Transitions.)

but the general characteristics of the  $\epsilon'(T, \omega)$  response were unaffected. The inset in Fig. 1 shows the effect of repeated measurements on  $\epsilon'$  at 1 bar and  $10^4$  Hz and suggests a tendency towards saturation. As already noted, the phase transition is first order accompanied by a discontinuous strain,<sup>5,6,9</sup> and the effect appears to be a strain-induced “aging” phenomenon.

### B. Influence of pressure on the dielectric response

Figure 2 shows a key result from the present work, namely, the large influence of pressure on the dielectric response as discussed in Ref. 13. The shift of the response to lower temperatures, the suppression of the amplitude of  $\epsilon'(T)$ , and the increase in the breadth of the *R* state (e.g., compare  $\Delta T$  for the 2- and 10-kbar isobars) are by now familiar pressure effects on perovskite relaxors.<sup>2,13</sup> Most interesting, however, is the expected vanishing of the spontaneous *R*-FE transition at  $T_c$  and the fact that the vanishing appears to occur at a lower pressure on cooling compared to heating. Thus, e.g., on cooling at 10 kbar the response is largely that of a relaxor with only a small vestige of this transition remaining (the region inside the circle in Fig. 2(b)) and the strong suggestion that it will completely vanish at a somewhat higher pressure. Unfortunately, the massive pressure apparatus could not be cooled below 295 K to identify where  $T_c$  vanishes.

Figure 3 shows the dielectric loss ( $\tan \delta$ ) data that go with

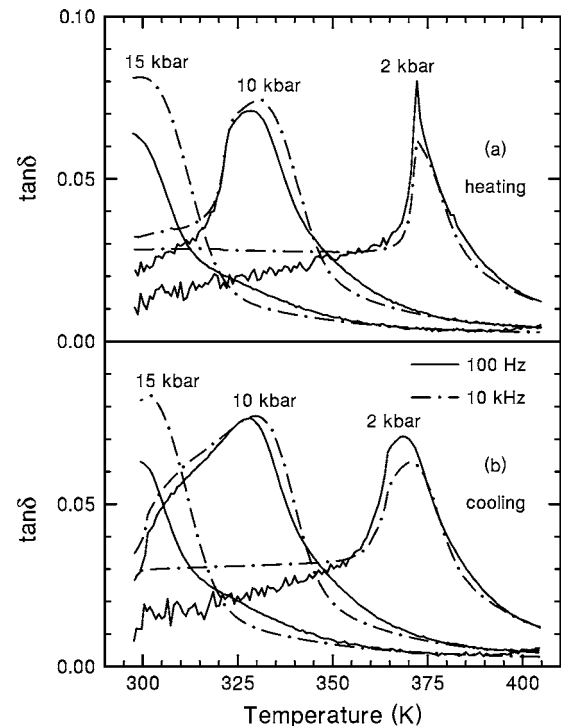


FIG. 3. Heating and cooling isobars of  $\tan \delta(T)$  for the same conditions as in Fig. 2. For clarity data at only  $10^2$  and  $10^4$  Hz are shown.

the real part in Fig. 2. These results show similar features as in Fig. 2. For clarity, we show data at fewer frequencies than in Fig. 2. With decreasing  $T$ , there is first, the broad increase in  $\tan \delta$ , followed by a sharp drop at  $T_c$ . The loss remains relatively low in the FE phase, a characteristic of ferroelectrics. The broader range of the *R* phase and its larger dielectric loss are evident in the data.

The isobaric measurements in Fig. 2 were complemented by the isothermal  $\epsilon'(P, \omega)$  results in Fig. 4.<sup>13</sup> These results mirror those in Fig. 2 and reveal effects with decreasing (increasing) temperature similar to those with increasing (decreasing) pressure. Specifically, with decreasing  $T$ , the pressure isotherms shift to higher pressures, the pressure range of the *R* state broadens, the discontinuity in  $\epsilon'$  at the *R*-FE transition decreases, and the transition broadens with the suggestion that it will vanish below 300 K. This is most clearly indicated by the region inside the circle for the 300 K isotherm in Fig. 4(b). Figure 5 shows the  $\tan \delta$  data that go with Fig. 4. For clarity we show data at only two frequencies ( $10^2$  and  $10^4$  Hz) for each isotherm.

### C. Temperature-pressure phase diagram

The  $T$ - $P$  phase diagram for PSN-*D* in Fig. 6 is unique and represents another key result of the present work. Although it was discussed in Ref. 13, we feel that a brief summary is worth repeating here. Plotted are  $T_m$  at  $10^4$  Hz and  $T_c$  on both heating and cooling at different pressures. There is a small thermal hysteresis in  $T_m$  (cooling data are shown in Fig. 6), but there is, of course, significant hysteresis in the first-order transition temperature represented by  $T_c$ . The data

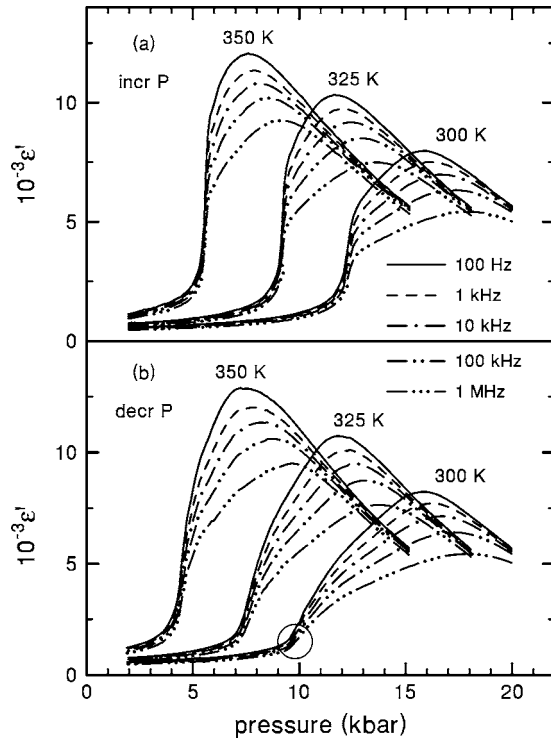


FIG. 4. Isotherms of  $\epsilon'$  versus pressure showing the influence of pressure on the dielectric response and phase behavior of PSN-D. (After Samara and Venturini, Ref. 13, with permission of Phase Transitions.)

points in Fig. 6 are from both isobaric and isothermal measurements with good agreement between the two. The increase in the separation (divergence) between the  $T_m(P)$  and  $T_c(P)$  phase boundaries with increasing pressure is a manifestation of the observed increase in the  $T$  range of the  $R$  phase with increasing pressure. The divergence of the two  $T_c(P)$  phase boundaries for increasing and decreasing  $T$  and  $P$  merely reflects the increased thermal hysteresis of the  $R$ -FE transition at higher pressures. The initial slopes in Fig. 6 are:  $dT_m/dP = -5.5$  K/kbar (at  $10^4$  Hz),  $dT_c/dP = -7.0$  K/kbar on heating, and  $dT_c/dP = -8.3$  K/kbar on cooling.

The above value of  $dT_m/dP$  for our PSN-D single crystal is significantly larger in magnitude than  $-4.5$  and  $-4.3$  K/kbar values reported by Yasuda and Fujita<sup>10</sup> for disordered and ordered ceramic samples, respectively. While their results suggest a smaller pressure derivative for the ordered ceramic, we believe that the two slopes are essentially the same when one takes into account experimental uncertainties including pressure calibration. Yasuda and Fujita's disordered ceramic sample did not exhibit the spontaneous  $R$ -FE transition seen in our PSN-D single crystal and in other single crystal<sup>5</sup> and disordered ceramic<sup>9</sup> samples.

In a recent paper Szafranski *et al.*<sup>11</sup> reported the influence of pressure on the dielectric response and on  $T_m$  and  $T_c$  of a "highly ordered" ceramic PSN sample. They observed a relaxor peak in  $\epsilon'(T)$  at 390 K under 1 bar and deduced  $dT_m/dP = -4.9$  K/kbar (at  $10^6$  Hz), in reasonable agreement with our value of  $-5.5$  K/kbar at  $10^4$  Hz. Their  $\epsilon'(T)$  response did not reveal an anomaly at  $T_c$ , but upon differenti-

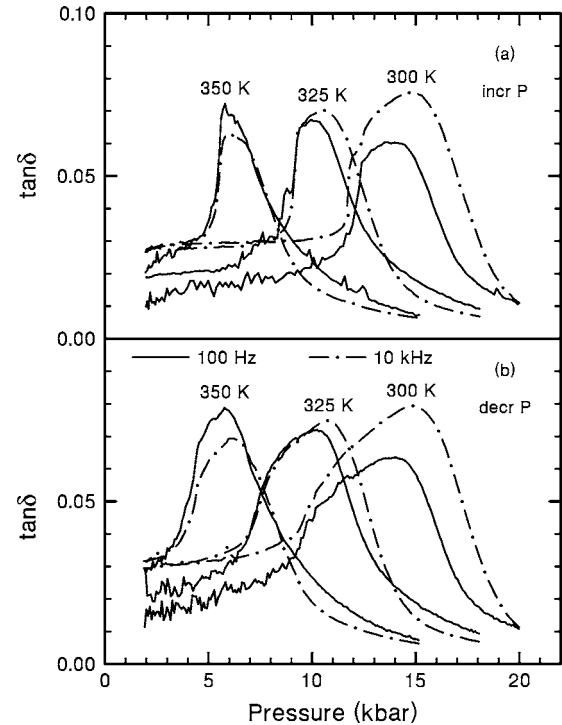


FIG. 5. Isotherms of  $\tan \delta$  versus pressure for the same conditions as in Fig. 4. For clarity, data at only  $10^2$  and  $10^4$  Hz are shown.

ating  $\epsilon'(T)$  with respect to  $T$ , a shoulder in the data was revealed. Assuming that this shoulder defines  $T_c$ , they report  $dT_c/dP = -3.8$  K/kbar, a value smaller in magnitude than  $dT_m/dP$ . On this basis, they suggest that the two-phase boundaries  $T_m(P)$  and  $T_c(P)$  may cross at some pressure beyond their range. Our results clearly show the opposite effect, i.e., the two boundaries diverge (see Fig. 6).

Because the  $R$ -FE phase transition is thermodynamically first order, the slope of  $dT_c/dP$  should be given by the Clausius-Clapeyron equation

$$dT_c/dP = \Delta V/\Delta S = T_c \Delta V/Q,$$

where  $\Delta V$  and  $\Delta S$  are the discontinuous changes in molar volume and entropy at  $T_c$ , and  $Q$  is the latent heat of the transition. The change in volume in going from the rhombohedral FE state to the cubic  $R$  state at  $T_c$  can be determined from the discontinuity in lattice parameters measured by neutron diffraction on a single crystal by Malibert *et al.*<sup>5</sup> The results yield  $\Delta V = -0.045$  cm<sup>3</sup>/mole. Using this value and our measured initial slope on heating,  $dT_c/dP = -7.0$  K/kbar, in the above equation yields  $\Delta S = 0.153$  cal/mole K and  $Q = 57$  cal/mole. Interestingly, these values are quite comparable to those of BaTiO<sub>3</sub> ( $\Delta S = 0.125$  cal/mole K and  $Q = 50$  cal/mole)<sup>14</sup> at its tetragonal FE-to-cubic paraelectric transition. These values of  $\Delta S$  are less than  $\frac{1}{4}$  those of typical order-disorder FE transitions [e.g., triglycine sulphate (TGS) and NaNO<sub>2</sub>]<sup>14</sup> and are, thus, more representative of displacive FE transitions.

The results in Figs. 2, 4, and 6 indicate that the  $R$ -to-FE transition will vanish at a pressure somewhat higher than

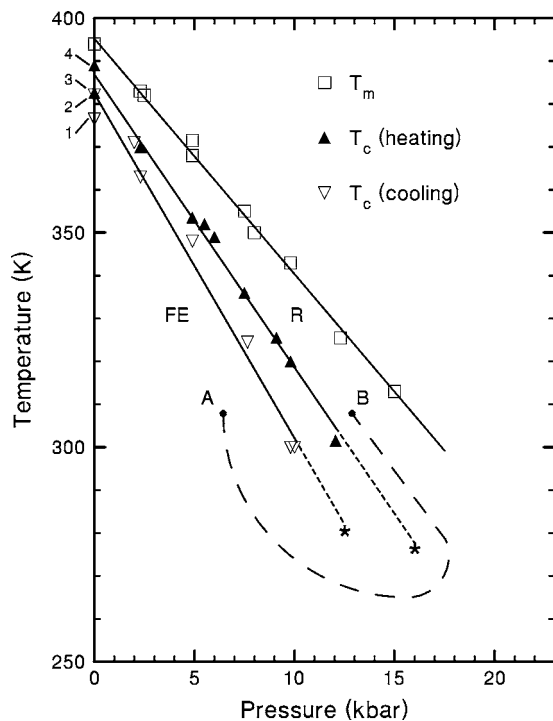


FIG. 6. Temperature-pressure phase diagram for the PSN-*D* crystal. An unusual feature is the expected termination of the  $T_c(P)$  phase boundaries (for both increasing and decreasing  $T$  and  $P$ ) at specific temperatures and pressures as somewhat arbitrarily denoted by the stars. The dashed curve defines a path for going from the FE (point A) to the R state (point B) continuously without crossing a phase boundary. The points labeled 1–4 for  $T_c$  at ambient  $P$  (1 bar) are as follows: points 1 and 2 are from the initial cooling or heating runs with our crystal (data in Fig. 1). Points 3 and 4 represent the average of seven cooling or heating runs at 1 bar after various runs under higher  $P$ . Points 1 and 2 fall somewhat below the extrapolation of the high- $P$  phase lines to 1 bar, suggesting a small pressure-seasoning effect on  $T_c$  (see the discussion of Fig. 1 inset in the text). (After Samara and Venturini, Ref. 13, with permission of Phase Transitions.)

represented by the 300 K data points in Fig. 6. This implies that each of the two  $T_c(P)$  phase boundaries in the phase diagram should terminate at a finite temperature and pressure, as somewhat arbitrarily depicted by the two stars. Such terminations in a phase diagram will normally represent critical points which, from a thermodynamic point of view, would be somewhat akin to the vapor-liquid critical point. A peculiar aspect in Fig. 6 is that there are two such critical pointlike features in the phase diagram of PSN-*D*, one on increasing  $T$  or  $P$  and the other on decreasing  $T$  or  $P$ .

In the present case, however, they simply represent cross-over phenomena whereby the R state evolves continuously from the FE phase with pressure.<sup>2,13</sup> This effect is due to the decrease in the correlation length (and thereby the size) of the polar nanoregions with compression. In addition to the vanishing of the  $\epsilon'(T)$  anomaly and  $T_c$  at the end points (stars), we expect the lattice distortion and the ionic displacements associated with the macroscopic rhombohedral phase to also vanish at these points, reverting the symmetry to cubic. A consequence of the results in Fig. 6 is that one can

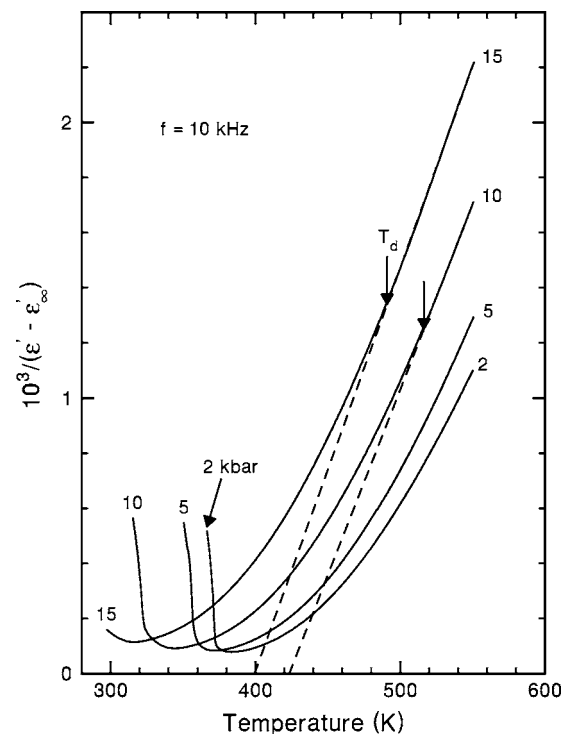


FIG. 7. Temperature dependence of  $1/\epsilon'$  at 2, 5, 10, and 15 kbar at  $10^4$  Hz, showing Curie-Weiss behavior above the Burns temperature,  $T_d$ , and strong deviations from this law below it.

reversibly follow a path such as that denoted by the dashed curve from the FE phase at point A to the R state at point B without crossing a phase boundary. This means that each state evolves from the other continuously. At temperatures below the expected end points (stars) in Fig. 6 and at higher pressures, only the R state should exist, consistent with earlier observations that this state is the ground state of disordered perovskites at high pressure (or reduced volume).<sup>2,12</sup>

We should note here that results based on the spherical random bond/random field theory of relaxors predict a feature in the phase diagram reminiscent of the critical pointlike features in Fig. 6.<sup>15</sup> Specifically, at low pressures the transition is from an ergodic relaxor state to the FE phase, whereas above the critical point only a nonergodic relaxor state exists. The theory was applied to the case of La-doped lead zirconate titanate (La/Zr/Ti=6/65/35) with good agreement with experimental results.<sup>12,15</sup> The behavior of PSN-*D* near the  $T_c(P)$  end points in Fig. 6 is sufficiently interesting that we hope to design a new pressure cell capable of higher pressures and lower temperatures than in Fig. 6 in order to study this region in some detail.

#### D. The high temperature Curie-Weiss response

As shown in Fig. 1, the  $\epsilon'(T)$  data above  $T_m$  deviate strongly from Curie-Weiss law, but it is expected that this law will be obeyed at sufficiently high  $T$ 's, as is common to many relaxors. Figure 7 shows that this is indeed the case for the PSN-*D* crystal. These results clearly show that there is a well-defined linear  $1/\epsilon'$  region for the 15-kbar and 10-kbar isobars over the range of  $T$  covered by the measurements. At

lower pressures, it is necessary to go to higher  $T$ 's to reach the linear regime. The  $T$  where the response in Fig. 7 deviates from linear defines the so-called Burns temperature,  $T_d$ .<sup>16</sup> This is the  $T$  where nanopolar domains in relaxors first make their presence known. The 10 and 15 kbar data yield  $T_d=516$  K and 493 K, respectively, so that  $dT_d/dP = -4.6$  K/kbar, a value close to that for  $dT_m/dP$ .

In the linear regimes, the results in Fig. 7 obey  $\varepsilon' = \varepsilon'_\infty + C/(T - T_0)$ . In this equation  $\varepsilon'_\infty$  is the high  $T$  limiting value of  $\varepsilon'$  which we take to be 75 (a different choice will not affect any of our conclusions). For the 10 and 15 kbar data,  $C = 7.5 \times 10^4$  K and  $6.8 \times 10^4$  K, and  $T_0 = 424$  K, and 400 K, respectively. Thus,  $dT_0/dP = -5.0$  K/kbar, i.e., comparable to that of  $dT_d/dP$ . The magnitude of  $C$  ( $\sim 1 \times 10^5$  K at 1 bar) is comparable to that of displacive perovskite ferroelectrics,<sup>14</sup> and its decrease with pressure is also typical of perovskite ferroelectrics.<sup>17</sup> For order-disorder ferroelectrics,  $C$  is typically  $\approx 1 \times 10^3$  K.

The deviation from Curie-Weiss law becomes more pronounced with decreasing  $T$  below  $T_d$  due to the growth of the polar nanodomains and the increase in their correlations in a manner similar to that of the  $T$  dependence of the magnetic susceptibility of spin glasses.<sup>2</sup> This growth can be represented by a  $T$ -dependent local-order parameter,  $q$ , as first suggested by Sherrington and Kirkpatrick<sup>18</sup> for spin glasses and adapted for PMN by Viehland *et al.*<sup>19</sup> The expression for  $q(T)$  can be written in the form

$$[1 - q(T)] = T\varepsilon'(T)/[C + T_0\varepsilon'(T)].$$

Analysis of the data in Fig. 7 shows that at 15 kbar,  $q$  grows from 0 at  $T_d$  to  $\sim 0.25$  at  $T_m$ , consistent with the growth of dipolar correlations.

### E. Dynamics of the dipolar freezing process

The frequency dispersion in the dielectric data in the  $R$  state provides a detailed view of the dynamics of the freezing of fluctuations of the polar nanodomains. The data define relaxation frequencies,  $\omega$  ( $=2\pi f$ , where  $f$  is the measuring frequency), corresponding to the peak temperatures,  $T_m$ , and characteristic relaxation times,  $\tau = 1/\omega$ . As is generally true of  $ABO_3$  relaxors, Fig. 8(a) shows that plots of  $\log \omega$  vs  $1/T_m$  are non-Arrhenius. This departure from the Arrhenius character is often analyzed in terms of the Vogel-Fulcher equation,

$$\tau^{-1} = \omega = \omega_0 \exp[E/k(T_m - T_O^*)],$$

which is applicable to many relaxational phenomena.<sup>2</sup>  $E$  is the energy barrier between equivalent dipolar orientations, and  $T_O^*$  is a reference temperature where all relaxation times diverge (and where the distribution of  $\tau$ 's becomes infinitely broad). Our experience has been that while we can certainly fit data such as those in Fig. 8(a) by this equation, it is essentially impossible to obtain unique fitting parameters  $\omega_0$ ,  $E$ , and  $T_O^*$  over a limited range (4-6 decades) of frequency. Data over a much broader range of frequencies are needed.<sup>2</sup> Nevertheless, an approximate fit [or just examining the data in Fig. 8(a)] suggests that  $E$  decreases with increasing pressure—a manifestation of the decrease in the size of the

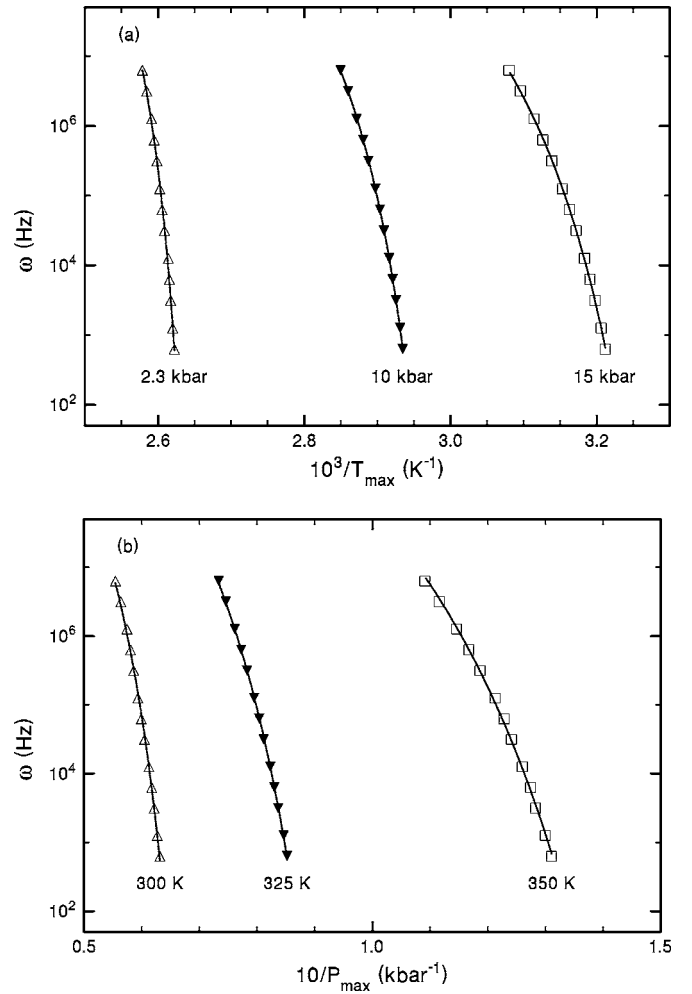


FIG. 8. Frequency dependence of the (a) temperature and (b) pressure relaxation maxima due to fluctuations of the polar nanoregions in the PSN- $D$  crystal, revealing the non-Arrhenius behavior.

polar nanodomains with pressure, as discussed below. Simply stated,  $E$  is proportional to the volume, and smaller polar domains are easier to reorient than larger ones, hence a lower  $E$ .

Figure 8(b) shows that isothermal data such as those in Fig. 4 yield a Vogel-Fulcher-like response in terms of pressure. Thus, the constant temperature  $\log \omega$  vs  $1/P_{\max}$  plots in Fig. 8(b) mirror the constant pressure  $\log \omega$  vs  $1/T_m$  plots in Fig. 8(a).

### F. Influence of dc bias

A biasing dc electric field can be expected to strongly influence the relaxational and FE responses of PSN. At low field, the field should favor the FE phase over the  $R$  state due to the enhancement of FE domains and their correlations, resulting in reduced frequency dispersion. The experimental results in Ref. 13, repeated here in Fig. 9 for the convenience of the reader, confirm this expectation. Using  $\Delta T$  to reflect the extent of the  $R$  range, the top inset shows that  $\Delta T$  decreases from 16 K at zero bias to  $\sim 10$  K at  $E = 2$  kV/cm (cooling data). The 4 kV/cm scan in Fig. 9 suggests that the

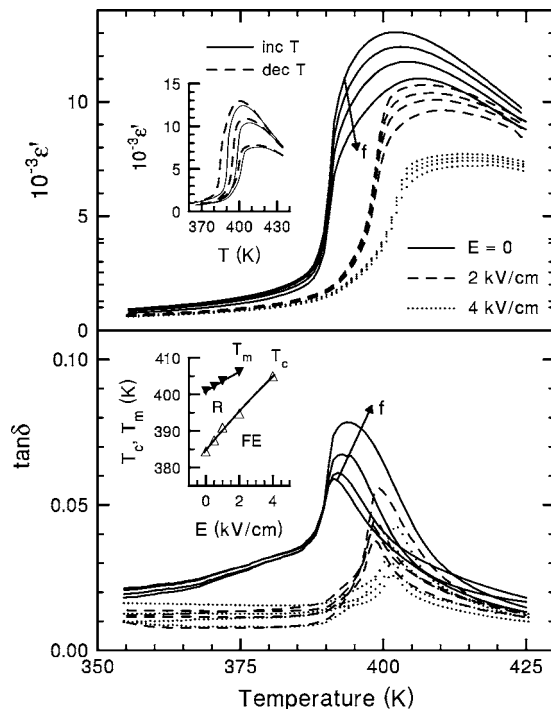


FIG. 9. The influence of dc electric field bias on the dielectric response of the PSN-D crystal at 1 bar on heating. The frequencies from left to right are  $10^3$  to  $10^6$  Hz by decades. The top inset shows the thermal hysteresis in  $\epsilon'(T)$  for the  $E=0$ , 2, and 4 kV/cm scans at  $10^4$  Hz and 1 bar. The lower inset shows the  $T$ - $E$  phase diagram at 1 bar ( $T_m$  at  $10^4$  Hz). (After Samara and Venturini, Ref. 13, with permission of Phase Transitions.)

$R$  state has essentially vanished. This is supported by the  $\tan \delta(T, \omega)$  response at 4 kV/cm in Fig. 9(b) and at 5 kV/cm in Fig. 10 which reflect the FE character. The evolution of the field effects at  $10^4$  Hz are shown in Figs. 9 and 10. The changes in  $\epsilon'(T)$  with a bias field in Fig. 9 are considerably larger than those reported by Yasuda and Fujita<sup>10</sup> for a disordered PSN ceramic.

Other field-induced effects in Figs. 9 and 10 are (i) a decrease in the sharpness of the FE transition, and (ii) a shift of  $T_c$  to higher temperatures. These effects are classic field-induced effects in ferroelectrics and are predicted from the Landau-Devonshire theory.<sup>14</sup> Qualitatively, the biasing field induces polarization in the high- $T$  phase, and this polarization merges gradually into the spontaneous polarization ( $P_s$ ) of the FE phase, so that there is no discontinuous change in  $P_s$  at  $T_c$ . The degree of smearing of the transition increases with the magnitude of  $E$ .

In the case of a first-order FE transition, as for our PSN-D crystal, a discontinuity in the spontaneous polarization, ( $\Delta P_s$ ), is still observed at low fields, but it occurs at  $T_c + \Delta T_c$ , i.e., above the zero field  $T_c$ . At higher fields the transition should become second-order where  $\Delta P_s \rightarrow 0$ , suggesting the existence of a tricritical point, as in the case of PMN crystal.<sup>20</sup> This is seen to be essentially the case for the PSN-D crystal at 5 kV/cm (see Fig. 10), or perhaps at slightly higher fields. Consistent with this picture, the thermal hysteresis of the FE transition should vanish above a certain field. Our results show that this hysteresis decreases from

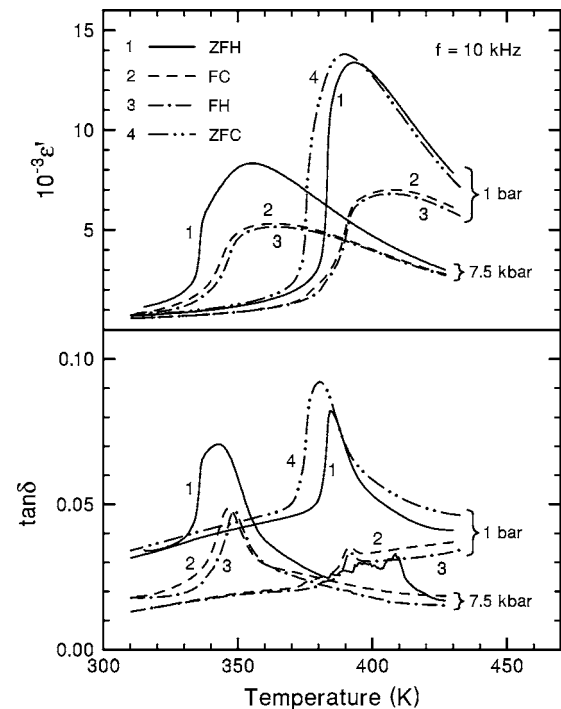


FIG. 10. A more detailed view of the influence of a 5 kV/cm dc bias on the dielectric response of the PSN-D crystal at 1 bar and 7.5 kbar at  $10^4$  Hz. The experimental sequence is denoted by the numbers 1, 2, 3, and 4 corresponding to zero-field heating (ZFH), field cooling (FC), field heating (FH), and zero-field cooling (ZFC), respectively. The “features” near 400 K in the ZFH  $\tan \delta$  data (curve 1) at 7.5 kbar are probably noise.

6 K at  $E=0$  to 1 K at 4 kV/cm and nearly vanishes at 5 kV/cm (Fig. 10).

Figure 10 provides a more detailed view of the influence of a biasing field on the dielectric response of PSN-D. Looking first at the 1 bar data, the experimental sequence was as noted by the numbers in the figure. Starting at 300 K, zero field heating (ZFH) yields curve 1 which is the familiar 1 bar response (see Fig. 1). This was followed by field cooling (FC, curve 2), field heating (FH, curve 3), and, finally, zero field cooling (ZFC, curve 4). The latter curve reproduces the original 1 bar response (see Fig. 1). The inset in Fig. 9 shows the  $T$ - $E$  phase diagram for PSN-D. Clearly the  $T$  range of the  $R$  state decreases with increasing  $T$ , and this state should vanish at some higher field. The 1 bar, 5 kV/cm data in Fig. 10 [especially  $\tan \delta(T)$ ] are suggestive of a full FE response.

Figure 10 also shows the influence of a 5 kV/cm field on the dielectric response at 7.5 kbar. Curves 1, 2, and 3 represent ZFH, FC, and FH, respectively. Because pressure favors the relaxor state, a field  $>5$  kV/cm is required to induce a full FE state at 7.5 kbar. This feature is evident in the data on Fig. 10 that show remaining vestiges in  $\epsilon'(T)$  and  $\tan \delta(T)$  of the  $R$  state at 7.5 kbar on contrasting the 1 bar and 7.5 kbar data.

### G. Mechanism for the relaxor/ferroelectric transitions

We shall now discuss the dielectric response of PSN-D with reference to Fig. 7. Above the Burns temperature,  $T_d$ ,

$\epsilon'$  ( $T$ ) obeys Curie-Weiss law with a Curie constant  $\sim 10^5$ , characteristic of displacive ferroelectrics.<sup>14</sup> It would be natural to suppose that this response is associated with a soft FE mode, but we are not aware of measurements that extend to sufficiently high  $T$  to confirm this. On the basis of pair-distribution-function analysis of pulsed neutron-diffraction measurements, Egami *et al.*<sup>7</sup> have identified off-center  $\text{Pb}^{2+}$  ion displacements in PST that decrease from 0.4 Å at 300 K to 0.25 Å at 750 K. The authors conclude that the polarization associated with these displacements is largely responsible for the dielectric behavior, and that the local polarization of  $\text{PbO}_{12}$  persists to temperatures well above  $T_d$ . This temperature is attributed to the order-disorder transition of the  $\text{Pb}^{2+}$  ion motion; above  $T_d$ , the  $\text{Pb}^{2+}$  displacements are dynamic and are not correlated.<sup>7</sup> In the absence of compositional disorder on the  $B$  sites, a ferroelectric transition might be expected at  $T_d$ ; however, the disorder on the  $B$  sites breaks long-range correlations and leads to the formation of polar nanodomains. A similar behavior can be expected for PSN- $D$ .

Once the polar nanodomains appear at  $T_d$ , there is an onset of relaxor behavior in PSN- $D$ , and the domains grow with increased correlations as  $T$  decreases. Associated with the increased correlations is an increase in the local-order parameter,  $q$ , as discussed in Sec. E above. Slowing down of the dipolar fluctuations of the nanodomains sets in at  $T_m$  and continues on decreasing  $T$ . However, growing correlations and, presumably, increase in the size of the nanodomains, ultimately results in the spontaneous onset of ferroelectric behavior and the formation of large domains at  $T \leq T_c$ .<sup>2</sup> This latter  $R \rightarrow \text{FE}$  transition in relaxors is usually induced by a biasing electric field,<sup>2</sup> but it is uniquely spontaneous (i.e., occurs at zero bias) in PSN and very few other materials (PST and certain PLZT compositions<sup>2</sup>).

X-ray diffuse scattering measurements on both ordered and disordered PSN have revealed insights into the physics near and below  $T_c$ .<sup>21</sup> In the ordered phase, the results reveal lattice instabilities at both the  $\Gamma$  and  $M$  points of the Brillouin zone that are characteristic of soft mode behavior and the formation of FE and antiferroelectric (AFE) phases, respectively. It is suggested that the coexistence of FE and AFE regions leads to frustration that results in the  $R$  state observed in the dielectric response.<sup>21</sup> In the case of the disordered sample, the scattering results reveal diffuse transition behavior at the two points, and there are no sharply defined phonons. Nevertheless, these scattering results revealed the basic soft-mode character of the ferroelectricity of PSN, consistent with our findings that the high-temperature Curie constant and entropy change at  $T_c$  reflect displacive behavior.

A recent NMR study<sup>22</sup> of the ionic displacements and polar ordering in PSN provides support for the diffuse scattering results<sup>21</sup> and for the earlier diffraction results.<sup>5-7</sup> Specifically, the NMR data reveal large (up to 0.4 Å) displacements of the  $\text{Pb}^{2+}$  ions and smaller (up to 0.1 Å) displacements of the  $\text{Sc}^{3+}$  ions along the four rhombohedral axes in agreement with the diffraction data. More importantly, the  $^{207}\text{Pb}$  and  $^{93}\text{Nb}$  NMR resonances detect a tetragonal AFE distortion of the PSN lattice in addition to the rhombohedral FE distortion below  $T_c$ . The tetragonal distortion appears at  $T_c$  and evolves continuously in a second-order

transition manner with decreasing  $T$ . Near  $T_c$  this distortion is very small and does not influence the rhombohedral distortion, but at  $T \leq 100$  K the two distortions become comparable. Thus, in agreement with the diffuse scattering results, the NMR data reveal the co-existence of two-order parameters in PSN associated with the condensation of two  $TO$  soft-modes, one of long and the other of short wavelength.<sup>22</sup> Soft-mode behavior would normally be also expected above  $T_c$ , but, in the presence of disorder and polar nanodomains in the  $R$  state, there are no well-defined phonon modes. In the  $R$  state the ionic displacements have much smaller correlation lengths than in the FE phase, and the ordered regions are simply polar nanodomains. Random fields and the AFE distortion prevent the formation of large FE domains. Evidence for the formation of polar nanodomains  $\sim 2$  nm in size has been revealed from TEM and x-ray diffraction (XRD) measurements on the isomorphous crystal PST.<sup>23</sup> Similar nanodomains can be expected in PSN.

There is increasing evidence that in many perovskites there is mixed displacive/order-disorder character to the dielectric response. In particular, for PST, and presumably PSN, the polar nanodomains originate from the correlated strongly anharmonic hopping motion of the  $\text{Pb}^{2+}$  ions (as noted above) in the presence of  $\text{Sc}^{3+}$  and  $\text{Ta}^{5+}$  ion disorder on the  $B$  sites.<sup>7,24</sup> It then follows that the flipping of the dipolar orientations of these domains contributes to the audio frequency dispersion observed in the  $R$  state.

Evidence also exists that in PST and some other relaxors a higher (microwave) frequency relaxation—a central mode, also contributes to the total dielectric response.<sup>24,25</sup> This relaxation has been attributed to the correlated motion of chains in the PST structure.<sup>25</sup> Both this relaxation and the lower-frequency relaxation, which is of our primary interest in this paper, disappear below  $T_c$ .

#### IV. CONCLUDING REMARKS

The present work has shown large effects of hydrostatic pressure and the dc biasing electric field on the dielectric properties and phase behavior of PSN- $D$ . These two variables have opposite effects, pressure favoring the  $R$  state and the biasing field favoring the FE phase. That pressure favors the  $R$  state was expected on the basis of earlier work which demonstrated that the  $R$  state is the ground state of compositionally disordered perovskites at reduced volume (high pressure).<sup>2,12</sup> This result can be simply understood by noting that pressure reduces the polarizability of the host crystal (as can be deduced from Fig. 2), thereby reducing the correlation length and size of the polar nanodomains, so that above a certain pressure there will not be sufficient correlations and overlap among the domains to precipitate an FE state. The electric field, on the other hand, strengthens dipolar correlations and leads to the formation of larger (FE) domains.

The  $T$ - $P$  phase diagram of PSN- $D$  is rather unusual in that the  $T_c(P)$  phase lines on both increasing and decreasing temperature and pressure appear to just terminate at specific end points in a manner akin to critical points. However, this behavior is believed to simply reflect an  $\text{FE} \rightarrow R$  crossover phenomenon. More detailed studies at somewhat higher pres-



tures (and lower temperatures) than reached in the present work is desirable to explore the regions denoted by stars in Fig. 6. In the  $T$ - $E$  plane, the  $T_m(\epsilon r)$  boundary in Fig. 9 should also terminate at an end point reflecting a  $R \rightarrow$  FE crossover.

#### ACKNOWLEDGMENTS

This work at Sandia National Laboratories was supported

by the Division of Materials Sciences and Engineering, Office of Basic Energy Sciences, U.S. Department of Energy. Sandia National Laboratories is operated by Sandia Corporation, a Lockheed Martin Company, for the DOE under Contract No. DE-AC04-94AL85000. The work at Simon Fraser University was supported by the U.S. Office of Naval Research (Grant No. N00014-99-1-0738).

- 
- <sup>1</sup>L. E. Cross, *Ferroelectrics* **76**, 241 (1987).  
<sup>2</sup>G. A. Samara, *Solid State Physics*, edited by H. Ehrenreich and F. Spaepen (Academic, New York, 2001), Vol. 56, p. 240 and references therein.  
<sup>3</sup>C. G. F. Stenger and A. J. Burggraaf, *Phys. Status Solidi A* **61**, 275 (1980).  
<sup>4</sup>P. Bonneau, P. Garnier, G. Calvarin, E. Husson, J. R. Gavarri, A. W. Hewat, and A. Morell, *J. Solid State Chem.* **91**, 350 (1991).  
<sup>5</sup>C. Malibert, B. Dkhil, J. M. Kiat, D. Durand, J. F. Bézar, and A. Spasojevic-de Biré, *J. Phys.: Condens. Matter* **9**, 7485 (1997).  
<sup>6</sup>C. Perrin, N. Menguy, E. Suard, Ch. Muller, C. Caranoni, and A. Stepanov, *J. Phys.: Condens. Matter* **12**, 7523 (2000).  
<sup>7</sup>T. Egami, E. Mamontov, and W. Dmowski, in *Fundamental Physics of Ferroelectrics 2003*, edited by P. K. Davies and D. J. Singh, AIP Conf. Proc. No. 677 (American Institute of Physics, Melville, NY, 2003), p. 48.  
<sup>8</sup>C. G. F. Stenger and A. J. Burggraaf, *Phys. Status Solidi A* **61**, 653 (1980).  
<sup>9</sup>F. Chu, I. M. Reaney, and N. Setter, *J. Appl. Phys.* **77**, 1671 (1995).  
<sup>10</sup>N. Yasuda and K. Fujita, *Ferroelectrics* **106**, 275 (1990).  
<sup>11</sup>M. Szafranski, A. Hilczler, and W. Nawrocik, *J. Phys.: Condens. Matter* **16**, 7025 (2004).  
<sup>12</sup>G. A. Samara, *Ferroelectrics* **274**, 183 (2002).  
<sup>13</sup>G. A. Samara and E. L. Venturini, *Phase Transitions* **79**, 21 (2006).  
<sup>14</sup>F. Jona and G. Shirane, *Ferroelectric Crystals* (Macmillan, New York, 1962).  
<sup>15</sup>R. Blinc, V. Bobnar, and R. Pirc, *Phys. Rev. B* **64**, 132103 (2001).  
<sup>16</sup>G. Burns and F. H. Dacol, *Phys. Rev. B* **28**, 2527 (1983).  
<sup>17</sup>G. A. Samara, in *Advances in High Pressure Research*, edited by R. S. Bradley (Academic Press, New York, 1969), Vol. 3, p. 174.  
<sup>18</sup>D. Sherrington and S. Kirkpatrick, *Phys. Rev. Lett.* **35**, 1972 (1975).  
<sup>19</sup>D. Viehland, M. Wuttig, and L. E. Cross, *Ferroelectrics* **120**, 71 (1991).  
<sup>20</sup>Z.-G. Ye, *Key Eng. Mater.* **155-156**, 81 (1998).  
<sup>21</sup>N. Takesue, Y. Fujii, M. Ichihara, H. Chen, S. Tatemori, and J. Hatano, *J. Phys.: Condens. Matter* **11**, 8301 (1999).  
<sup>22</sup>V. V. Laguta, M. D. Glinchuk, I. P. Bykov, R. Blinc, and B. Zalar, *Phys. Rev. B* **69**, 054103 (2004).  
<sup>23</sup>I. M. Reaney, J. Petzelt, V. V. Voitsekhovskii, F. Chu, and N. Setter, *J. Appl. Phys.* **76**, 2086 (1994).  
<sup>24</sup>E. Buixaderas, S. Kamba, and J. Petzelt, *Ferroelectrics* **308**, 131 (2004).  
<sup>25</sup>F. Chu, N. Setter, C. Elissalde, and J. Ravez, *Mater. Sci. Eng., B* **38**, 171 (1996).